

Monolayer g-C₃N₄ Fluorescent Sensor for Sensitive and Selective Colorimetric Detection of Silver ion from Aqueous Samples

Yujuan Cao^{1,2} · Wei Wu¹ · Song Wang¹ · Hong Peng¹ · Xiaogang Hu^{1,2} · Ying Yu^{1,2}

Received: 10 November 2015 / Accepted: 5 January 2016 / Published online: 11 January 2016
© Springer Science+Business Media New York 2016

Abstract Rapid and sensitive detection of heavy-metal ions in natural water environments worldwide is urgently needed because of their severe threats to human health. In the present work, monolayer graphite-like flake C₃N₄ (g-C₃N₄) materials were applied as a new fluorescent sensor for the detection of trace silver ion in aqueous solution. The thickness of synthesized g-C₃N₄ was 0.45 nm and obtained by exfoliating twice with ultrasonic. With the presence of ethylene diamine tetraacetic acid as a screening agent, the highly sensitive sensor reached a low detection limit of 52.3 nmol/L for silver (I) ion and there was no disturbance when silver (I) ion coexisted with other metal ions in water samples. Under the optimal conditions, the monolayer g-C₃N₄ was successfully used to detect trace silver (I) ion in different environmental water and drinking water samples.

Keyword Monolayer g-C₃N₄ · Fluorescent sensor · Silver (I) ion · Aqueous samples

Introduction

Silver is not only the most ancient metal with numerous applications in the fields like jewelry, coins, mirrors, anti-corrosive alloys, but also an important element used in

electroplating, photographic and imaging industries. Moreover, the products containing silver nanoparticles are the most applicable nanomaterials in the last decade because of their excellent antibacterial activity and have been widely used in various fields including textiles, food containers, and medical devices [1]. The rapidly growing use of silver inevitably releases large amounts of soluble silver species to the environment and may cause environmental problems. It has been found that silver is toxic for humans at a concentration higher than 0.9 mmol/L in drinking water. Excessive intake of silver ions (Ag⁺) causes argyria in humans and silver deposition has been found in the skin, gingival, cornea, liver, and kidney of patients [2]. For these reasons, determination of trace amount of silver ions with high sensitivity, specificity and rapidity in environmental and industrial samples has great importance.

Various instrumental techniques have been employed for the determination of silver species in different real samples, including atomic absorption spectroscopy (AAS) [3], inductively coupled plasma–mass spectrometry (ICP-MS) [4], inductively coupled plasma optical emission spectrometry and flow injection analysis [5]. However, these techniques need highly sophisticated instruments and a complex preparation process, which are not applicable in most cases. Optical sensing systems have been gained great attention for the effective and sensitive detection. Various organic compounds, quantum dots, nanoparticles, polymers and DNA have been used as chemosensors [6]. For examples, fluorescence switch that consists of DNA-templated silver nanoclusters [7] or nanographene carbon composite potentiometric sensor for the determination of trace amounts of silver (I) ion were recently fabricated and the detection limits were lower to 4.17×10^{-9} mol/L [8]. Room temperature cation exchange reaction in nanocrystals were used to amplify the signal and the detection limit of Ag⁺ using ICP-MS was 0.3 pg/L [9]. Although these methods show high sensitivity for Ag⁺

✉ Yujuan Cao
caoyj@scnu.edu.cn

¹ School of Chemistry and Environment, South China Normal University, Guangzhou 510006, China

² Guangzhou Key Laboratory of Analytical Chemistry for Biomedicine, South China Normal University, Guangzhou 510006, China

detection, they have several drawbacks such as laborious synthesis of reagents, complex detection system, etc. The development of convenient and direct method for the assay of silver in different real samples is still in an urgent need.

Fluorescence spectroscopy is a commonly method for the detection of organic pollutants [10] or heavy metal ions [11], etc. The majority of fluorescent probes commonly using metal nanoparticles require modification and from their own toxicity considerations. In recent years, low-toxic graphene carbon nitrogen compounds ($g\text{-C}_3\text{N}_4$) fluorescent porous material much attention and numerous studies have been devoted to synthesizing and designing highly functional $g\text{-C}_3\text{N}_4$ materials [12]. Due to their unique catalytic, electrical conductivity and adsorption properties, $g\text{-C}_3\text{N}_4$ materials have been successfully applied as photocatalysts for the degradation of organic dyes in water under light irradiation [13]. It is also an environment-friendly and biocompatibility fluorescence materials for bioimaging and biomedical applications [14]. Unlike other sensors with optical receptor hooking on the porous materials, $g\text{-C}_3\text{N}_4$ itself is the receptor and thus performs higher sensitivity. Lee et al. [15] had studied feasibility of detecting trace amount Cu^{2+} in aqueous solution with $g\text{-C}_3\text{N}_4$ as optical sensor via observing its photoluminescence quenching effects and the limit of detection (LOD) of Cu^{2+} in aqueous solution was 12.336 nmol/L. Subsequently, Barman and his coworkers [16] explored $g\text{-C}_3\text{N}_4$ quantum dots as optical sensor to detect mercuric and iodide ions via a mechanism terms namely “ON-OFF-ON” and the lower LOD for Hg^{2+} was about 10^{-9} mol/L. Another turn on fluorescence sensor, Cu^{2+} -cubic mesoporous $g\text{-C}_3\text{N}_4$, was also developed for detection of CN^- and its LOD in both aqueous solution and human blood serum was 80 nmol/L [17]. However, its excellent chemical resistance emerged in the work done by Gillan [18] showed that $g\text{-C}_3\text{N}_4$ was almost insoluble in water, ethanol, toluene, diethyl ether and THF, which may be due to the van der Waals between its layers stacking. Recently, studies had shown that the use of liquid exfoliating method can also obtained nanosheets structure, but the synthesis needs more than 10 h [19, 20].

Herein, we prepared monolayer $g\text{-C}_3\text{N}_4$ by using liquid exfoliating method with ultrasonic oscillating for twice. The obtained monolayer $g\text{-C}_3\text{N}_4$ shows good selective fluorescent response to Ag^+ and it was then utilized as a fluorosensor to detect Ag^+ in aqueous solutions in the presence of other metal ions.

Experiments

Reagents and Apparatus

Reagents Dicyandiamide (Aladdin, Shanghai, China), ferric nitrate, barium nitrate, beryllium nitrate, mercury nitrate, potassium nitrate, manganese nitrate, zinc nitrate, chromium nitrate, cadmium nitrate, silver nitrate, lead nitrate, copper nitrate, cobalt nitrate,

aluminum nitrate, nickel nitrate, magnesium nitrate and ethylene diamine tetraacetic acid (EDTA) were purchased from Guangzhou Chemical Reagent Ltd. (Guangzhou, China). All reagents were used directly. Ultra-pure water used throughout the whole experiments was obtained from the MILLI-Q gradient A10 system (Millipore, Bedford, MA, USA).

Apparatus The fluorescence intensity (FL) was performed by Hitachi F-2500 fluorescence spectroscopy. UV-vis spectroscopy was recorded on a TianMei UV-VIS 1700 spectrophotometer. The Fourier transform infrared spectroscopy (FT-IR) experiment was carried out on a Shimadzu Prestige-21 FT-IR spectrometer in a KBr pellet, scanning from 4000 to 400 cm^{-1} at room temperature. Atomic force microscopy (AFM) study was performed by means of Veeco DI nanoscope Multi Mode V system. X-ray diffraction (XRD) patterns of the $g\text{-C}_3\text{N}_4$ was obtained on a Philips X ray diffractometer (PW 3040/60) using $\text{Cu K}\alpha$ target at 40 kV and 40 mA. Scanning electron microscopy (SEM) was performed with a Hitachi S-4800 scanning electron microanalyzer using an accelerating voltage of 15 kV.

Preparation of the Bulk $g\text{-C}_3\text{N}_4$ Porous Materials

The bulk $g\text{-C}_3\text{N}_4$ was prepared by directly pyrolysis of dicyandiamide in a porcelain crucible. In detail, five grams (5.0 g) of dicyandiamide was added into a porcelain crucible and placed in a muffle furnace (Shanghai, China); Then it was heated at $520\text{ }^\circ\text{C}$ for 4 h under air condition with a ramp rate of about $4.5\text{ }^\circ\text{C}/\text{min}$ for both the heating and cooling processes. In order to obtain the finally bulk $g\text{-C}_3\text{N}_4$, the obtained yellow powder was further heated at $500\text{ }^\circ\text{C}$ in another porcelain crucible for 2 h with a ramp rate of $2.3\text{ }^\circ\text{C}/\text{min}$.

Preparation of Monolayer $g\text{-C}_3\text{N}_4$ Materials

The monolayer $g\text{-C}_3\text{N}_4$ materials were prepared by a liquid exfoliating method. In brief, 50.0 mg of bulk $g\text{-C}_3\text{N}_4$ powder was dispersed in 100 mL of water with ultrasonic dispersion for 2 h. The formed $g\text{-C}_3\text{N}_4$ suspension was then centrifuged at 5000 rpm to remove the unexfoliated bulk $g\text{-C}_3\text{N}_4$ and a stable $g\text{-C}_3\text{N}_4$ suspension can be obtained. And then, the obtained $g\text{-C}_3\text{N}_4$ suspension was further exfoliated with ultrasonic for 2 h. A stable monolayer $g\text{-C}_3\text{N}_4$ material with highly water-dispersivity was obtained and it can be kept for months without depositing.

Fluorescence Measurements

The fluorescence measurement of Ag^+ was performed at room temperature. 1.0 mL monolayer $g\text{-C}_3\text{N}_4$ was added into an aqueous solution with V_1 mL silver ion and V_2 mL of water, wherein $V_1 + V_2 = 1.0\text{ mL}$. And then, it was measured triplicate according to the requirements.

For the interference tests, 1.0 mL of monolayer $g\text{-C}_3\text{N}_4$ were mixed with 0.01 mL 1.65 $\mu\text{mol/L}$ silver ion solution and 0.05 mL interference ions with the same concentration of Ag^+ , then 0.01 mol/L EDTA was added into this mixed solution and diluted to 2.0 mL to obtain the finally sample solution. After 2.0 min, the PL intensity was measured and all of experiments were test for triplicate.

All of the water samples were filtered with a 0.45 μm membrane filter, and then measured as the same process of interference tests.

The value of LOD was calculated as $\text{LOD} = 3\sigma/S$, where σ is the standard deviation of PL intensity of monolayer $g\text{-C}_3\text{N}_4$ at 435 nm in the absence of Ag^+ and S is the slope between PL intensity at 435 nm versus Ag^+ concentration.

Results and Discussion

AFM measurement was carried out to understand the thickness of obtained monolayer $g\text{-C}_3\text{N}_4$ and the results are shown in Fig. 1a and 1b. As can be seen from Fig. 1b, the randomly

measured nanosheets were nearly 0.45 nm of thickness. This value of the thickness was as same as that of grapheme reported before [21], indicating the exfoliated nanosheets are comprised of only C – N monolayer.

XRD analysis was also carried out to investigate the crystal structure of the samples. As shown in Fig. 1c, two characteristic peaks of bulk $g\text{-C}_3\text{N}_4$ could be observed. One is the strong peak at 27.6° corresponding to the (002) plane, which is attributed to the interlayer distance $d = 0.33$ nm in bulk $g\text{-C}_3\text{N}_4$. The other is the week peak at 13.2° corresponding to the (100) plane, which is related to the inplane structural packing motif of tri-s-triazine units. For the monolayer $g\text{-C}_3\text{N}_4$, the significant decrease in the peak at 27.6° can be attributed to the reduced correlation length introduced by nanostructuring [22].

Further evidence for the $g\text{-C}_3\text{N}_4$ phase comes from the FT-IR spectra and the results are showed in Fig. 1d. The board peaks between 3000 to 3500 cm^{-1} corresponded to the N–H stretching and hydrogen-bonding interactions. The peaks at 1101 and 1633 cm^{-1} were contributed to the typical stretching

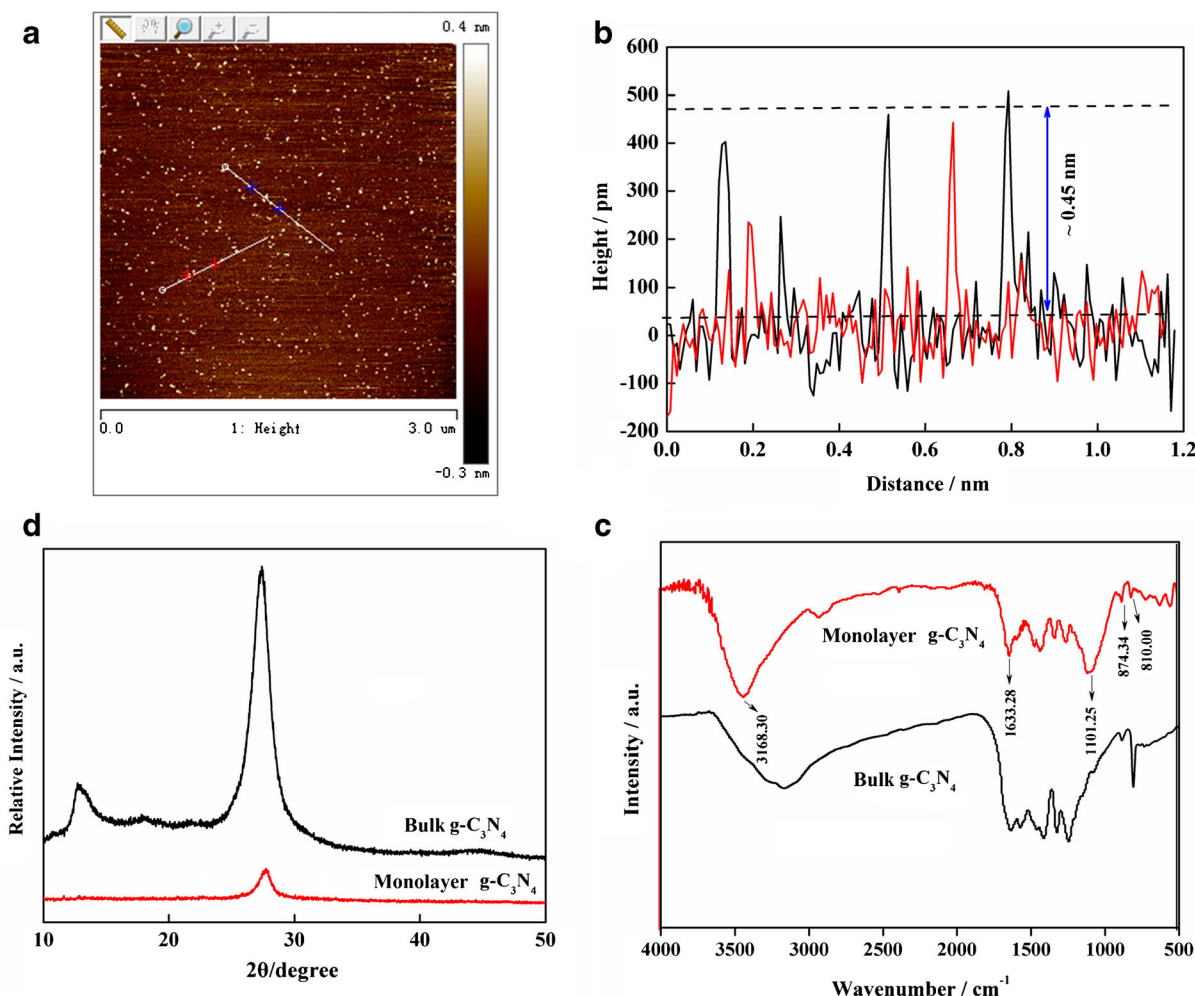
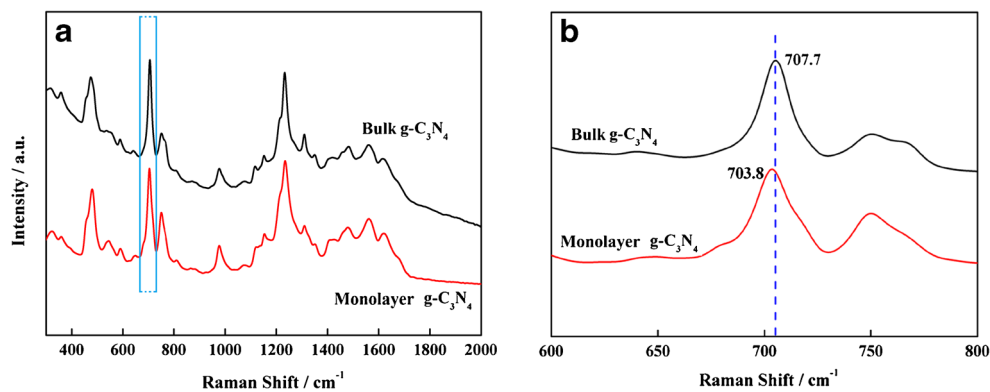


Fig. 1 Characterizations of monolayer $g\text{-C}_3\text{N}_4$. AFM image (a & b), XRD spectrum (c) and the FT-IR spectrum (d)

Fig. 2 Raman spectra of the bulk $g\text{-C}_3\text{N}_4$ (black line) and the monolayer $g\text{-C}_3\text{N}_4$ (red line)



vibration of connected units of $\text{C-N}(\text{-C})\text{-C}$ (full condensation) or C-NH-C (partial condensation), while the absorption band located at about 810 cm^{-1} was originated from the vibration of triazine ring. It is worth noting that there were no differences of FT-IR peak between the bulk $g\text{-C}_3\text{N}_4$ and the monolayer $g\text{-C}_3\text{N}_4$, which indicated that the chemical structure of the monolayer $g\text{-C}_3\text{N}_4$ was as same as that of the bulk $g\text{-C}_3\text{N}_4$.

In addition, Raman spectra were also carried out to study the structure changes between as-exfoliated monolayer $g\text{-C}_3\text{N}_4$ and bulk counterpart. As can be seen from Fig. 2, the Raman spectrum of as-exfoliated $g\text{-C}_3\text{N}_4$ nanosheets showed nearly identical Raman shifts of bulk $g\text{-C}_3\text{N}_4$, indicating the exfoliated ultrathin $g\text{-C}_3\text{N}_4$ nanosheets retain the same crystal structure of bulk $g\text{-C}_3\text{N}_4$. Comparing with bulk $g\text{-C}_3\text{N}_4$, the Raman spectra of monolayer $g\text{-C}_3\text{N}_4$ nanosheets showed a blue shift of about 4 cm^{-1} (Fig. 2b), ascribing to the phonon confinement effect of the as-exfoliated nanosheets and inferring their ultrathin thickness. At the same time, both of the Raman spectra of bulk $g\text{-C}_3\text{N}_4$ and monolayer $g\text{-C}_3\text{N}_4$ nanosheets show no shifts of carbon materials, which often located at about 1350 cm^{-1} and 1580 cm^{-1} , indicating the high purity of the as-exfoliated nanosheets.

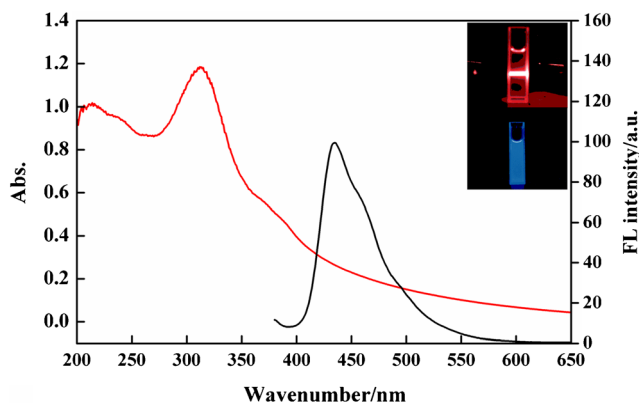


Fig. 3 UV-vis absorbing (red line) and fluorescence spectra (black line) of the monolayer $g\text{-C}_3\text{N}_4$ and its Tyndall effect exhibition

The monolayer $g\text{-C}_3\text{N}_4$ exhibited exceptional solubility in water and the solution were stable for several weeks without any precipitation. Its optical properties were examined in the solution. Figure 3 shows the monolayer $g\text{-C}_3\text{N}_4$ has a strong absorption at 312 nm in UV light; A strong fluorescence peak centered at 435 nm was observed when the aqueous solution was excited at 365 nm . The nearly transparent feature as well as the well-defined Tyndall effect of the monolayer $g\text{-C}_3\text{N}_4$ solution as displayed in the inset of Fig. 3 indicate the presence of highly monodisperse monolayer nanosheets in water.

The selectivity of the monolayer $g\text{-C}_3\text{N}_4$ towards Ag^+ and other different metal ions in water was investigated. The change in fluorescence intensity (FL) before and after the addition of interfering ions by five times of molar concentrations to the Ag^+ solution of $1.65\text{ }\mu\text{mol/L}$ are shown in Fig. 4a. Comparing to $g\text{-C}_3\text{N}_4 + \text{Ag(I)}$, the FL differences of $g\text{-C}_3\text{N}_4 + \text{M(n)}$ (Fe^{3+} , Ba^{2+} , Be^{2+} , Hg^{2+} , K^+ , Mn^{2+} , Zn^{2+} , Pb^{2+} , Cr^{3+} , Mg^{2+} , Ni^{2+} , Co^{2+} , Ca^{2+} , Cd^{2+} and Al^{3+}) were much lower, indicating no significant spectral change of monolayer $g\text{-C}_3\text{N}_4$ observing in the presence of these interface ions. But after the silver (I) ion was added into the solution of $g\text{-C}_3\text{N}_4 + \text{M(n)}$, significant FL differences ($g\text{-C}_3\text{N}_4 + \text{M(n)} + \text{Ag(I)}$) were observed and the intensities were similar to that of $g\text{-C}_3\text{N}_4 + \text{Ag(I)}$. The quenching of FL response of monolayer $g\text{-C}_3\text{N}_4$ with various metal ions clearly shows the selectivity of Ag^+ to bind with it. However, it was reported that the PL intensity of $g\text{-C}_3\text{N}_4$ could be gradually quenched with increasing Cu^{2+} concentration [15]. In the present work, a decrease about 25 % in the PL intensity was also observed when Cu^{2+} coexisted with other cations.

EDTA is the most widely used chelator in analytical chemistry, which forms strong 1:1 complexes with many metal ions. Most of the formation constants for EDTA complexes are larger than 10^{10} and trend to be larger for more positively charged cations [23]. For example, the formation constant for Cu^{2+} of $10^{18.8}$ is much larger than that for Ag^+ ($10^{7.3}$), indicating the interference of Cu^{2+} in the present work can be eliminated by EDTA. Figure 4b presents the quenching results of monolayer $g\text{-C}_3\text{N}_4$ with Ag^+ and Cu^{2+} in the presence of EDTA. For the tests, $1.65\text{ }\mu\text{mol/L}$ Ag^+ ion and $8.25\text{ }\mu\text{mol/L}$

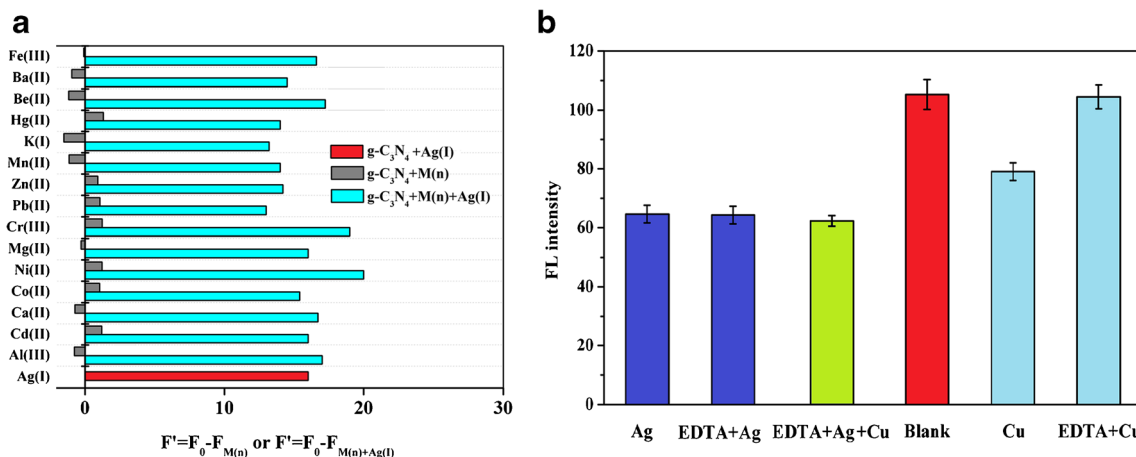


Fig. 4 Selective FL response of monolayer g-C₃N₄ without EDTA, upon adding 1.65 μmol/L Ag⁺, and upon adding 8.25 μmol/L other metal ion solutions (a); FL response of monolayer g-C₃N₄ with 0.01 mol/L EDTA,

upon adding 1.65 μmol/L Ag⁺, 8.25 μmol/L Cu²⁺ solutions, respectively, and upon adding both Ag⁺ and Cu²⁺ solutions (b)

Cu²⁺ were used to quench the PL intensity of monolayer g-C₃N₄ in the presence of 0.01 mol/L EDTA. The PL intensity of monolayer g-C₃N₄ was significantly quenched when Ag⁺ was added into the system, and similar results were also observed when the EDTA was present as chelator, suggesting that the added EDTA showed slight influence on the quench of PL intensity for Ag⁺. On the other hand, although the PL intensity of monolayer g-C₃N₄ was also obviously quenched when Cu²⁺ was added into the system, a slightly quenching was obtained in the presence of EDTA. Further experiments on the test of PL intensity of monolayer g-C₃N₄ with Ag⁺, Cu²⁺ and EDTA also confirmed that the interference of Cu²⁺ can be successfully eliminated.

In order to evaluate the sensitivity, the PL changes were monitored with increasing concentration of Ag⁺ ion. As shown in Fig. 5, the intensity of the PL emission centered at

435 nm is highly sensitive to Ag⁺ and decreases with an increasing concentration of Ag⁺. The relative PL intensity ($F' = F_0 - F$, where F_0 and F are fluorescence intensities at 435 nm in the absence and presence of Ag⁺ ions) showed good linear correlation when the concentration of Ag⁺ increased from 0.16 to 1.65 μmol/L. The correlation coefficient (R^2) was more than 0.99 and the relative standard deviation (RSD) was lower than 5%. The limit of detection was as low as 52.7 nmol/L at a signal-to-noise ratio of 3.0, which is about 8 times lower than the maximum level of Ag⁺ in drinking water permitted by the World Health Organization (WHO).

In order to evaluate whether the monolayer g-C₃N₄ based fluorescent sensor was applicable as a real diagnostic system, different samples including environmental water and drinking water samples were analyzed. The samples were analyzed immediately after filtration with a 0.45 μm membrane filter. The results showed that no Ag⁺ was detected in these samples probably because their concentrations were far below the limit of detection of the proposed method. Good recoveries of the spiked Ag⁺ in these samples with different levels ranging from 80.8% to 115.8% were obtained and the results are shown in Table 1.

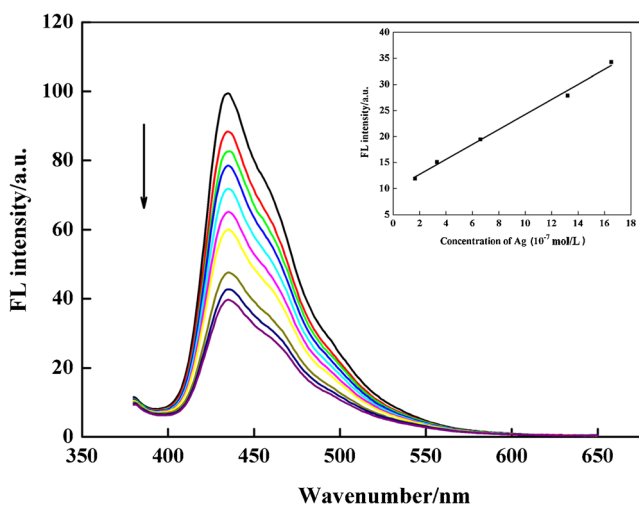


Fig. 5 a fluorescence spectra of g-C₃N₄ monolayer nanosheets dispersion in the presence of different Ag⁺ concentrations; The insert is the dependent of $F' = F_0 - F$ on the concentrations of Ag⁺ ions ranging from 0.165 to 1.65 μmol/L

Table 1 Application of monolayer g-C₃N₄ on the detection of Ag⁺ in aqueous samples

Samples	Recovery (% , n = 3) of different spiked samples		
	0.33 μmol/L	0.66 μmol/L	1.65 μmol/L
Rainwater	102.3 ± 4.1	97.4 ± 4.0	115.8 ± 5.1
Tap water	102.2 ± 3.9	80.8 ± 3.2	98.5 ± 4.7
Mineral water	114.9 ± 5.3	115.2 ± 3.6	98.6 ± 4.1
Lake water	93.1 ± 3.7	105.4 ± 4.5	113.9 ± 2.1

Conclusions

In summary, although the bulk g-C₃N₄ had showed good sensitive PL response to Cu²⁺ without interference by other metal ions including Ag⁺, the monolayer g-C₃N₄ showed more selective and sensitive to the Ag⁺ than the Cu²⁺. On the application of monolayer g-C₃N₄ fluorescence sensor, the interference of Cu²⁺ coexisting in the samples can be simply screened by adding EDTA chelant. Under such an optimal conditions, the monolayer g-C₃N₄ can be successfully used to detect trace Ag⁺ in real water samples.

Acknowledgments We are grateful to Dr. Xiao-hua Xiao from Sun Yat-sen University for his helpful advice. This work was supported by the National Natural Science Foundation of China (No.21275056).

References

- Dastafkan K, Khajeh M, Ghaffari-Moghaddam M, Bohlooli M (2015) Silver nanoparticles for separation and preconcentration processes. *TrAC-Trends Anal. Chem.* 64:118–126
- Greulich C, Braun D, Peetsch A, Diendorf J, Siebers B, Epple M, Koller M (2012) The toxic effect of silver ions and silver nanoparticles towards bacteria and human cells occurs in the same concentration range. *RSC Adv* 2:6981–6987
- Mohammadi SZ, Afzali D, Heshmati Z (2013) Ligand-less in situ surfactant-based solid phase extraction for preconcentration of silver from natural water samples prior to its determination by atomic absorption spectroscopy. *Toxico. Environ. Chem.* 95:1299–1308
- Poitras EP, Levine MA, Harrington JM, Essader AS, Fennell TR, Snyder RW, Black SL, Sumner SS, Levine KE (2015) Development of an analytical method for assessment of silver nanoparticle content in biological matrices by inductively coupled plasma mass spectrometry. *Biol Trace Elem Res* 163:184–192
- Zhang JF, Zhou Y, Yoon J, Kim JS (2011) Recent progress in fluorescent and colorimetric chemosensors for detection of precious metal ions (silver, gold and platinum ions). *Chem Soc Rev* 40:3416–3429
- Singha S, Kim D, Seo H, Cho SW, Ahn KH (2015) Fluorescence sensing systems for gold and silver species. *Chem Soc Rev* 44:4367–4399
- Lee J, Park J, Lee HH, Park H, Kim HI, Kim WJ (2015) Fluorescence switch for silver ion detection utilizing dimerization of DNA-Ag nanoclusters. *Biosens. Bioelectron.* 68:642–647
- Afkhami A, Shirzadmehr A, Madrakian T, Bagheri H (2015) New Nano-composite potentiometric sensor composed of graphene nanosheets/thionine/molecular wire for nanomolar detection of silver ion in various real samples. *Talanta* 131:548–555
- Huang K, Xu KL, Tang J, Yang L, Zhou JR, Hou XD, Zheng CB (2015) Room temperature cation exchange reaction in nanocrystals for ultrasensitive speciation analysis of silver ions and silver nanoparticles. *Anal Chem* 87:6584–6591
- Xu WG, Wang X, Cai ZW (2013) Analytical chemistry of the persistent organic pollutants identified in the Stockholm convention: a review. *Anal Chim Acta* 790:1–13
- Vazquez-Gonzalez M, Carrillo-Carrion C (2014) Analytical strategies based on quantum dots for heavy metal ions detection. *J. Biomed. Optics* 19:101503
- Li XF, Li M, Yang JH, Li XY, Hu TJ, Wang JS, Sui YR, Wu XT, Kong LN (2014) Synergistic effect of efficient adsorption g-C₃N₄/ZnO composite for photocatalytic property. *J. Phy. Chem. Solids* 75:441–446
- Li YH, Sun YJ, Dong F, Ho WK (2014) Enhancing the photocatalytic activity of bulk g-C₃N₄ by introducing mesoporous structure and hybridizing with graphene. *J. Colloid Interf. Sci.* 436:29–36
- Zhang XD, Xie X, Wang H, Zhang JJ, Pan BC, Xie Y (2013) Enhanced photoresponsive ultrathin graphitic-phase C₃N₄ nanosheets for bioimaging. *J Am Chem Soc* 135:18–21
- Lee EZ, Jun YS, Hong WH, Thomas A, Jin MM (2010) Cubic mesoporous graphitic carbon(IV) nitride: an all-in-one chemosensor for selective optical sensing of metal ions. *Angew Chem Int Ed* 49:9706–9710
- Barman S, Sadhukhan M (2012) Facile bulk production of highly blue fluorescent graphitic carbon nitride quantum dots and their application as highly selective and sensitive sensors for the detection of mercuric and iodide ions in aqueous media. *J Mater Chem* 22:21832
- Lee EZ, Lee SU, Heo NS, Stucky GD, Jun YS, Hong WH (2012) A fluorescent sensor for selective detection of cyanide using mesoporous graphitic carbon (IV) nitride. *Chem Commun* 48:3942–3944
- Wang Y, Wang XC, Antonietti M (2012) Polymeric graphitic carbon nitride as a heterogeneous organocatalyst: from photochemistry to multipurpose catalysis to sustainable chemistry. *Angew Chem Int Ed* 51:68–89
- Tian JQ, Liu Q, Asiri MA, Al-Youbi AO (2013) Ultrathin graphitic carbon nitride nanosheet: a highly efficient fluorosensor for rapid, ultrasensitive detection of Cu²⁺. *Anal Chem* 85:5595–5599
- Zhang XL, Zheng C, Guo SS, Li J, Yan H, Chen G (2014) Turn-on fluorescence sensor for intracellular imaging of glutathione using g-C₃N₄ nanosheet–MnO₂ sandwich nanocomposite. *Anal Chem* 86:3426–3434
- Novoselov KS, Geim AK, Morozov SV, Jiang D, Zhang Y, Dubonos SV, Grigorieva IV, Firsov AA (2004) Electric field effect in atomically thin carbon films. *Science* 306:666–669
- Goettmann F, Fischer A, Antonietti M, Thomas A (2006) Chemische synthese von mesoporösen kohlenstoffnitriden in harten templatens und ihre anwendung als metallfreie katalysatoren in friedel-crafts-reaktionen. *Angew Chem* 118:4579–4583
- Haris DC (2010) Quantitative chemical analysis (8th). Clancy Marshall, NY